FEBS Letters 588 (2014) 4701–4707

journal homepage: www.FEBSLetters.org

Kinetics of the early events of GPCR signalling

Roslin J. Adamson, Anthony Watts *

Biomembrane Structure Unit, Biochemistry Department, University of Oxford, South Parks Road, Oxford OX1 3QU, UK

ARTICLE INFO

Article history:
Received 14 August 2014
Revised 10 October 2014
Accepted 27 October 2014
Available online 11 November 2014

Edited by Christian Griesinger

Keywords:
G protein-coupled receptor
Electron microscopy
Surface plasmon resonance
Nanodisc
G protein

ABSTRACT

Neurotensin receptor type 1 (NTS1) is a G protein-coupled receptor (GPCR) that affects cellular responses by initiating a cascade of interactions through G proteins. The kinetic details for these interactions are not well-known. Here, NTS1-nanodisc-$G\alpha_s$ and $G\alpha_{i1}$ interactions were studied. The binding affinities of $G\alpha_{i1}$ and $G\alpha_s$ to NTS1 were directly measured by surface plasmon resonance (SPR) and determined to be 15 ± 6 nM and 31 ± 18 nM, respectively. This SPR configuration permits the kinetics of early events in signalling pathways to be explored and can be used to initiate descriptions of the GPCR interactome.

1. Introduction

G protein-coupled receptors (GPCRs) constitute a large and diverse family of seven transmembrane receptors. Around 800 of these, the class A GPCRs, mediate responses of the cell to external stimuli such as hormones, photons, small molecules and peptides, through interactions with heterotrimeric G proteins. Ligand binding initiates a cascade of cell signalling events, beginning with a conformational change in the receptor that activates heterotrimeric G proteins. After activation by the receptor, Gα exchanges guanosine diphosphate (GDP) for guanosine triphosphate (GTP) in its binding pocket. Gα and Gβγ dissociate and signal through binding partners and second messengers to effect cellular response through diverse effectors, including adenylyl cyclase (AC), GTPases, phospholipase C proteins (PLCs), phosphoinositide 3-kinase (PI_3K) and Ca^{2+} channels. Gα hydrolyses GTP to GDP and reassociates into the inactive heterotrimer with Gβγ. The signalling potential of GPCRs is amplified by their ability to bind various Gαβγs, which additionally may be composed of various combinations of the 21 Gα, 6 β, or 12 γ subunits [1].

The GPCR neurotensin receptor type 1 (NTS1) binds neurotensin (NT), a 13 amino acid peptide (ELYENKPRRPYIL) that acts as a neurotransmitter in the brain and as a local hormone in peripheral organs, with high affinity (K_D ~1 nM) [2,3]. NTS1 signals primarily through G_q, which binds intracellular loop 3 of NTS1, but also through the inhibitory G_{i1} and the stimulatory G_s, which bind near the C-terminus of the receptor [4]. NT modulates varied physiological responses, including appetite, stress and anxiety, analgesia [5], thermoregulation [6], maternal care [7] and dopaminergic signalling [2]. It thus plays an important role in conditions such as Parkinson's disease, eating disorders, psychosis, drug addiction, pain and has also been implicated in colon cancer.

The only high-resolution structural knowledge of GPCR-G protein interactions is from the β_2 adrenergic receptor-G protein complex structure solved by Rasmussen et al. [8], and the crystal structure of agonist-bound NTS1 was solved only recently [9]. Standard functional assays involving downstream effectors or radioactive GTPγS G protein activation to describe GPCR-G protein interactions do not assay the protein-protein interfacial interactions directly. Quantitative kinetic data of GPCR-G protein interactions comes from studies of the interactions of δ and μ-opioid receptors with G proteins using plasmon waveguide resonance [10–12]. Here, receptors were embedded in black lipid membranes (BLM) in order to mimic closer the native environment of the receptors. Few studies of the interactions of NTS1 with G proteins

Abbreviations: AC, adenylate cyclase; CHAPS, 3-[(3-cholamidopropyl)dimethylammonio]-1-propanesulfonate; CHS, cholesteryl hemisuccinate; DDM, dodecyl-β-D-maltoside; EDTA, ethylenediamine tetraacetic acid; FLAG-NTS1, FLAG-tagged NTS1; GDP, guanosine diphosphate; GTP, guanosine triphosphate; GPCR, G protein-coupled receptor; IPTG, isopropyl β-D-1-thiogalactopyranoside; NTS1, neurotensin receptor type 1; PI_3K, phosphoinositide 3-kinase; PLC, phospholipase C; POPC, 1-palmitoyl-2-oleoyl-*sn*-glycero-3-phosphocholine; POPE, 1-palmitoyl-2-oleoyl-*sn*-glycero-3-phosphoethanolamine; POPG, 1-palmitoyl-2-oleoyl-*sn*-glycero-3-phospho-(1′-*rac*-glycerol); RU, response units; SCK, single cycle kinetics

* Corresponding author.
E-mail address: anthony.watts@bioch.ox.ac.uk (A. Watts).

http://dx.doi.org/10.1016/j.febslet.2014.10.043
0014-5793/

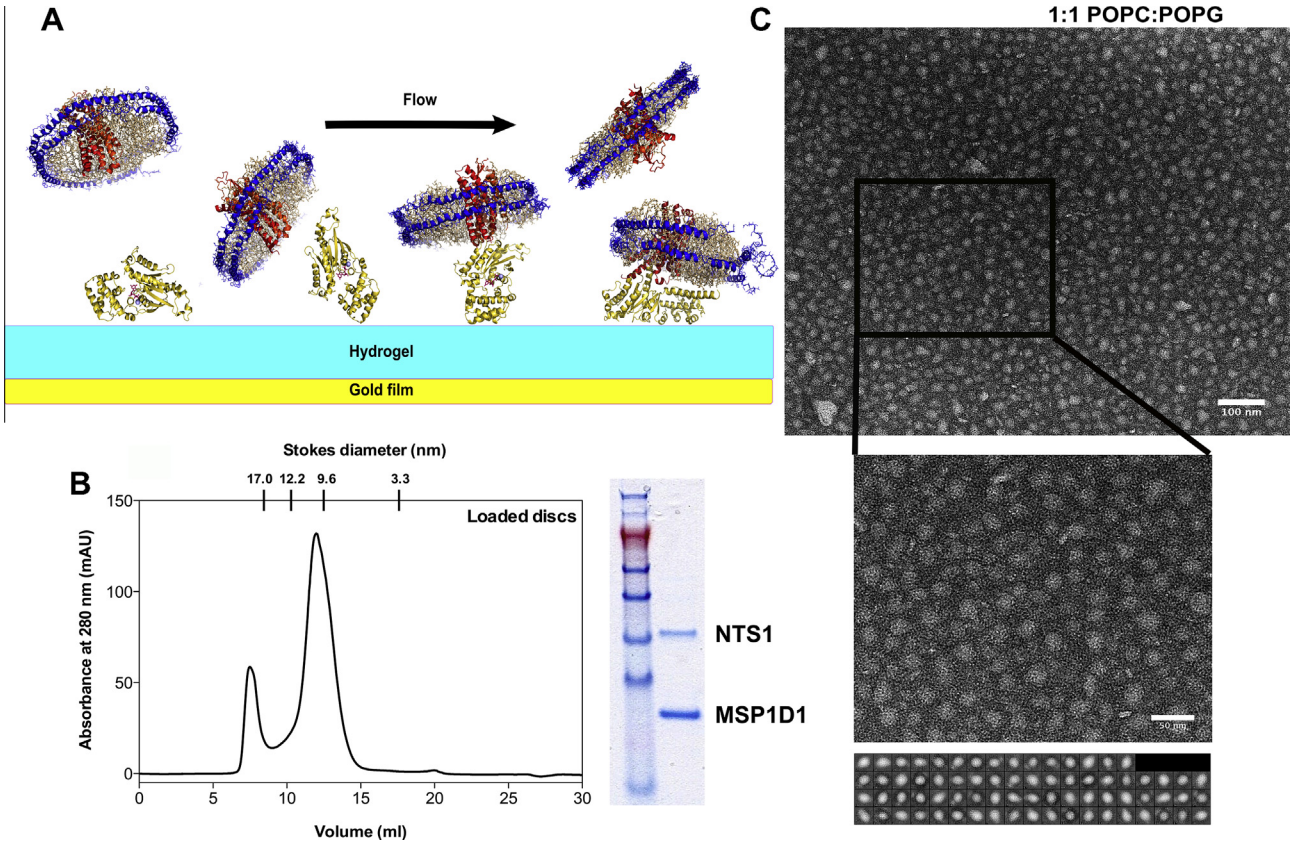

Fig. 1. Nanodisc preparation and NTS1-G protein coupling determination. (A) Schematic representation of the experimental setup. G proteins (gold) were amine-coupled to a CM5 Biacore chip (GE Healthcare). FLAG-NTS1-loaded nanodiscs were injected over the sample and reference flow cells. The reference flow cell was activated and blocked or ovalbumin was amine-coupled to it. Empty discs were injected over the sample and reference flow cells as a reference. Single cycle kinetics using serial concentrations of FLAG-NTS1-nanodiscs was performed. Data were double-referenced. (B) Representative SEC profile for nanodisc purification. A peak composed of large aggregates and vesicles elutes in the void volume at approximately 7.5 ml, followed by the nanodisc peak at ~12.5 ml, corresponding to a calibrated size of approximately 10 nm (left). SDS–PAGE of anti-FLAG enriched nanodiscs, showing approximately twice the amount of MSP1D1 compared to NTS1, which understains with Coomassie Brilliant Blue (right). (C) Negative stain EM images showing nanodisc sample. Nanodiscs prepared with a 1:1 ratio of POPC:POPG form homogeneous populations. Stain was 2% uranyl acetate. Reference-free class averages of 10–12 nm PC:PG discs (prepared using EMAN2 [54]) are shown. Box size is 18.5 nm. Scale bars are 100 nm (upper) and 50 nm (lower).

have been reported (all assayed by activation of the G protein) [4,13,14], and little is known of any of the kinetics of the subsequent signalling events. An understanding of the kinetics of interaction of GPCR receptors with their cognate G proteins, preferably under conditions that mimic the native lipid environment of the receptors, is essential for drug development that targets signalling pathways. Structural information and the determination of the affinity of binding would narrow the field of potential drug targets.

We have used surface plasmon resonance (SPR) to investigate the interactions of the α subunits of G_{i1} and G_s with NTS1 reconstituted into 10-nm size lipid discs termed nanodiscs [15,16]. This avoids common problems encountered when studying membrane proteins using this method, such as detergent and glycerol giving rise to artefactual signals, whilst additionally enabling the study of the receptor in specific lipid mixes. To our knowledge, this is the first time that the G protein binding kinetics of a peptide-binding GPCR in a lipid membrane environment have been determined using SPR, and the first time that a GPCR in nanodiscs has been used as the analyte in SPR studies.

2. Materials and methods

2.1. Materials

Dodecyl-β-D-maltoside (DDM), 3-[(3-cholamidopropyl)dimethylammonio]-1-propanesulfonate (CHAPS) were purchased from Melford Laboratories and cholesteryl hemisuccinate (CHS) from Sigma. Palmitoyl-oleoyl phosphatidylcholine (POPC) and palmitoyl-oleoyl phosphatidylglycerol (POPG) were from Avanti Polar Lipids. All other reagents were analytical grade.

2.2. Protein expression and purification

2.2.1. NTS1B purification

The NTS1B fusion construct has been described previously [17,18]. The construct was modified to contain a FLAG tag (DYKDDDDK). NTS1B was expressed and purified as described previously [19], but phospholipids were omitted from the buffers and 10% glycerol was used in the final elution from the affinity column. TEV cleavage and affinity purification of cleaved NTS1 were performed as described [19,20]. Approximately 1.0 mg FLAG-NTS1 was obtained from 80 g cells.

2.2.2. MSP1D1 purification

The Membrane Scaffold Protein 1D1 (MSP1D1) construct was obtained from AddGene (Addgene plasmid 20061) [16]. The protein was expressed and purified according to [21] with modifications. Briefly, the protein was expressed at 37 °C using BL21(DE3) *Escherichia coli* cells (Calbiochem) in 2 L flasks containing 500 ml TB medium inoculated with 5 ml starter culture prepared as described, until the OD_{600} reached 1.6. Expression was induced with 1 mM IPTG and the cells were harvested by centrifugation

(8000×*g*; 15 min). MSP1D1 purification was performed as described, with the exception that a cocktail of 2 μg/ml pepstatin A, 2 μg/ml leupeptin and 3 μg/ml aprotinin were used instead of phenylmethylsulfonyl fluoride (PMSF).

2.2.3. G protein purification

The constructs for the alpha subunits of G_s and G_{i1} were kindly donated by Renaud Wagner (University of Strasbourg, France). Gα subunits were expressed and purified according to [22], with minor modifications. The His-tagged proteins were expressed using *E. coli* BL21(DE3) cells (Calbiochem) and purified using metal affinity chromatography on a 5 ml HisTrap High Performance column (GE Healthcare). $G\alpha_{i1}$ was eluted from the column using a linear gradient of imidazole from 10 mM to 150 mM imidazole over 15 ml. $G\alpha_s$ was eluted from the column in 10 mM steps up to 150 mM over 160 ml.

2.2.4. FLAG-NTS1 reconstitution into nanodiscs

The protocols for reconstitution of membrane proteins into nanodiscs were followed in initial reconstitution attempts [15,16,21,23–26], but optimal ratios of MSP:FLAG-NTS1 and MSP:lipid were empirically determined. MSP:FLAG-NTS1 mol ratios of both 80:1 or 50:1 yielded fractions of homogeneously-sized nanodiscs, confirmed with negative stain electron microscopy (EM). The lipid:MSP ratio for either a 1:1 mix of POPC:POPG or a 3:1:1 mix of POPC:POPE:POPG with 25 mol% cholesterol was 65:1 for empty discs and 60:1 for loaded discs. Final concentrations of all components were approximately 160 μM MSP1D1, 8 mM lipid, 3 μM FLAG-NTS1, 16 mM sodium cholate, 2.6% glycerol. For empty discs, the volume of the reaction mixture was brought up to the same volume as the FLAG-NTS1 sample with the same DDM-containing buffer as FLAG-NTS1.

A calibrated Superdex 200 10/300 GL size exclusion column (GE Healthcare) was equilibrated in 50 mM Tris–HCl, pH 7.4, 100 mM NaCl, 5 mM $MgCl_2$. Homogeneously-sized nanodiscs were separated from larger vesicles and aggregates at a flow rate of 0.4 ml/min.

Receptor-containing nanodiscs were enriched through the use of an anti-FLAG antibody column according to the directions (anti-FLAG M2 agarose, Sigma–Aldrich). Receptor-containing nanodiscs were eluted using 100 μg/ml FLAG® peptide (F3290, Sigma–Aldrich), dialysed extensively against Nanodisc SPR buffer (50 mM Tris–HCl, pH 7.4, 100 mM NaCl, 5 mM $MgCl_2$), and concentrated to ~1 μM using 100 000 MWCO Vivaspin centrifugal concentrator tubes (Sartorius).

2.2.5. Surface plasmon resonance

SPR was performed on a Biacore T100 instrument later upgraded to a T200 (GE Healthcare). Single cycle kinetics (SCK) were performed due to no suitable regeneration conditions being found for multiple cycles. $G\alpha_s$ or $G\alpha_{i1}$ were amine-coupled to the carboxymethylated surface of a CM5 chip (Biacore, GE Healthcare) using standard protocols. Briefly, G proteins were dialysed into 40 mM sodium phosphate buffer, pH 7.4 with 5 mM $MgCl_2$. The calculated p*I* values for His-$G\alpha_{i1}$ and His-$G\alpha_s$ were 6.1 and 6.0

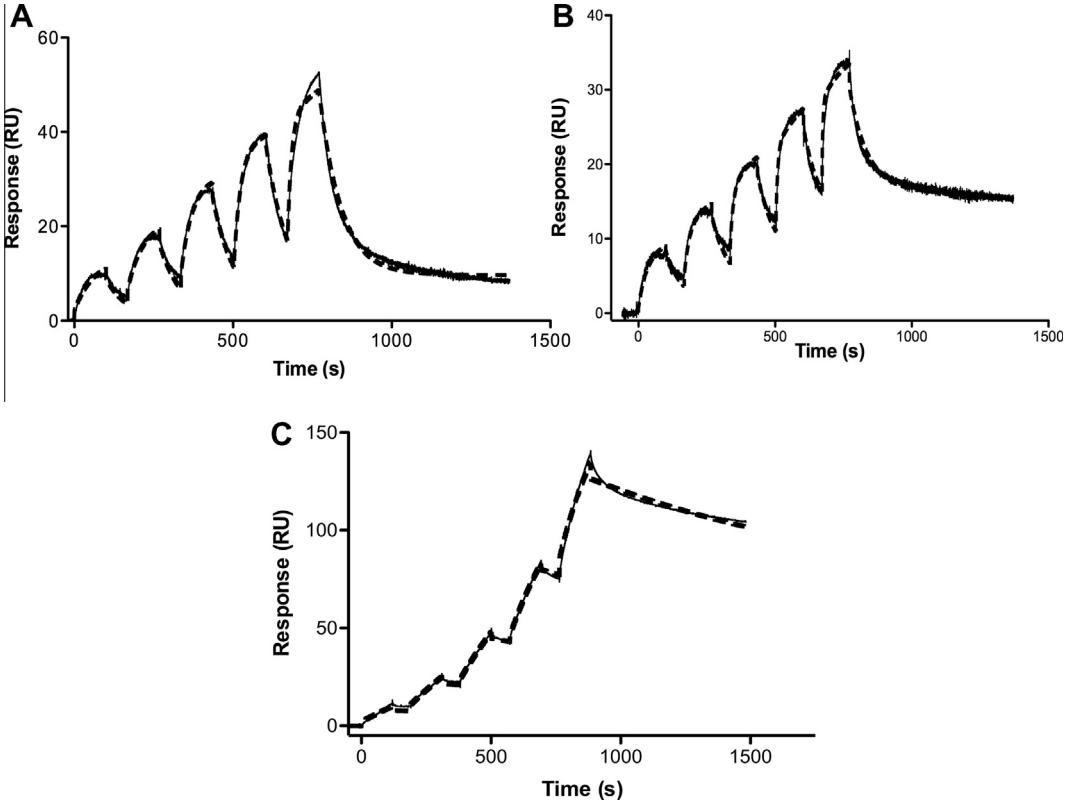

Fig. 2. SPR traces of GPCR G coupling. (A) and (B) FLAG-NTS1-PC:PG nanodiscs coupling to His_6-G_s or His_6-G_{i1} immobilised on a CM5 chip. Approximately 7000 RU G_s was amine-coupled to a CM5 Biacore chip (GE Healthcare) in 10 mM sodium acetate, pH 5.5 (A). Approximately 13000 RU G_{i1} was amine-coupled to a CM5 Biacore chip (GE Healthcare) in 10 mM sodium acetate, pH 5.0 (B). The reference flow cell was activated and blocked. Serial concentrations of 41.25–660 nM (A) and 25–400 nM (B) nanodisc-reconstituted and ligand-bound FLAG-NTS1 were injected over the chip surface. Empty nanodiscs at the same concentrations were injected as a reference, and data were double-referenced. The affinity of G_s (A) for FLAG-NTS1 in nanodiscs was 9 nM in this instance, and 9 nM for G_{i1} (B). (C) His_6-G_s coupling to FLAG-NTS1-PC:PG nanodiscs captured on an L1 chip. FLAG-NTS1-PC:PG nanodiscs (2500 RU) and empty PC:PG nanodiscs (2000 RU) were captured in FC 4 and 3, respectively, of an L1 chip by an 800-s injection at 5 μl/min. The chip was thoroughly washed in running buffer at 50 μl/min for 30–60 min. Serial dilutions of 1000 nM (62.5, 125, 250, 500, 1000 nM) His_6-G_s were injected across the flow cells for 150 s per concentration at 50 μl/min. The data (solid lines) were fitted with a 1:1 Langmuir binding model as well as a heterogeneous ligand binding model (dashed lines), giving K_D values of 65 nM for the 1:1 fit and 0.5 and 80 nM for K_{D1} and K_{D2} respectively. The χ^2 values for the fits were 4.4 and 3.3, respectively.

Table 1
Averaged kinetic parameters for Gα coupling to FLAG-NTS1-PC:PG nanodiscs.

	His_6-$G\alpha_s$			His_6-$G\alpha_s$ with GTPγS			His_6-$G\alpha_{i1}$		
	Mean	SEM[a]	N[b]	Mean	SEM	N[b]	Mean	SEM	N[b]
k_{a1} (M^{-1} s^{-1})	1.9×10^5	1.9×10^3	12	1.4×10^5	680	4	3.2×10^5	340	6
k_{d1} (s^{-1})	2.4×10^{-3}	4.2×10^{-5}	12	1.7×10^{-3}	5.4×10^{-5}	4	1.1×10^{-2}	8.4×10^{-6}	6
K_{D1} (nM)	31	18	12	72	23	4	15	6	6
k_{a2} (M^{-1} s^{-1})	4.6×10^5	3.0×10^4	10	8.9×10^4	1.8×10^3	4	1.4×10^5	2.8×10^3	6
k_{d2} (s^{-1})	4.4×10^{-1}	7.5×10^{-3}	10	7.3×10^{-2}	5.1×10^{-4}	4	1.6×10^{-2}	1.1×10^{-4}	6
K_{D2} (nM)	470	130	10	880	160	4	330	170	6
R_{max1}	29	16	12	30	22	4	29	15	6
R_{max2}	33	10	10	21	4.6	4	37	15	6

A one-tailed *t*-test comparing His_6-$G\alpha_s$ with GTPγS and His_6-Gαi1 with His_6-$G\alpha_s$ in pairs established that there were no significant differences between either of the two paired datasets ($p > 0.05$).
[a] Standard error of the mean.
[b] Number of experiments.

respectively (http://web.expasy.org/protparam). Coupling was most efficient at pH 5.0 for His-$G\alpha_{i1}$ and pH 5.5 for His-$G\alpha_s$, as determined by pH scouting on an unmodified chip surface. G proteins were diluted to 10 μg/ml in 10 mM sodium acetate pH 5.0 or 5.5. The chip was primed in HBS-N (10 mM HEPES, 150 mM NaCl, pH 7.4) and normalised with normalising solution (GE Healthcare). Coupling was as follows at 10 μl/min: 2 × 60 s injections of 50 mM NaOH, 420 s injection of NHS/EDC, 1000 s injection of Gα at appropriate pH, and finally the surface was blocked with a 420 s injection of ethanolamine. The reference flow cell was either simply activated and blocked with 2 × 60 s injections of 50 mM NaOH, 420 s injection of NHS/EDC, and 420 s injection of ethanolamine, or ovalbumin was amine-coupled to the surface as above, with 840 s injection of 10 μg/ml in 10 mM sodium acetate, pH 4.0. The chip was extensively washed at 50 μl/min for 1–2 h, then primed in Nanodisc SPR buffer. NT-bound (NT in excess (5 μM)), anti-FLAG-enriched NTS1-nanodiscs and empty nanodiscs were serially diluted five times from 660 nM or 400 nM. SCK programmes were performed at 30–50 μl/min, using the empty nanodiscs as a buffer reference. Three 60 s start-up injections of Nanodisc SPR buffer were followed by serial injections of nanodiscs for 90–120 s. Fig. 1A shows a schematic diagram of the experiment.

Data were confirmed by switching the roles of nanodiscs and Gα subunits to ligand (the surface-bound molecule in SPR terminology) and analyte (in solution) respectively.

SPR data was analysed using the BiaCore T100 or T200 BiaEvaluation software (Biacore). Data was double-referenced and 1:1 and heterogeneous ligand binding fits were applied.

3. Results

3.1. Nanodisc formation

Nanodisc formation efficiency depended on the lipid:MSP1D1:NTS1 ratio. Lower amounts of lipid were required when higher ratios of NTS1 incorporated into discs were needed. High ratios of MSP1D1:FLAG-NTS1 (50:1 mol:mol) were used to ensure insertion of primarily monomers into the nanodiscs. Assuming a Poisson distribution of FLAG-NTS1 into the discs [27], with this 50:1 ratio over 96% of discs would be empty, 3.8% would contain one receptor, and less than 0.08% would contain two receptors. After enrichment of loaded nanodiscs using the FLAG tag on NTS1 and an anti-FLAG column, 2% of discs would contain two receptors. In all cases though, some level of large aggregates was present in the nanodisc reaction mixture, which was separated from the homogeneous nanodisc population using SEC (Fig. 1B). The peak fractions corresponding to a disc size of ~10 nm were pooled, anti-FLAG purified if required, concentrated and dialysed. As expected, the discs contained twice the amount of MSP1D1 as NTS1, and were pure on gels (Fig. 1B). EM confirmed size homogeneity of the populations (Fig. 1C). Specific activity of the NTS1-nanodiscs was determined at ~5% by a radioligand binding assay.

Diameters for the FLAG-NTS1-loaded PC:PG-containing discs were 10 nm, and slightly smaller for the PPPC-containing discs at 9.5 nm. Empty discs tended to be smaller (~0.6 nm) than the respective loaded discs. The diameters of nanodiscs calculated from the standards of a calibrated gel filtration column correspond to average molecular masses of approximately 200 ± 15 kDa for the loaded PC:PG discs, and for empty discs, 10–20 kDa less. Correspondingly, PPPC discs were 160–180 kDa, with empty discs up to 15 kDa lighter. The Stoke's radius assumes a spherical particle, thus overestimating the mass of a disc-shaped object, and so the number of lipid molecules calculated from the area of the disc is likely to be lower than that calculated for the molecular mass. Taking the PC:PG discs as an example, and using lipid areas of 0.56 nm^2 for POPG and 0.66 nm^2 for POPC [28], subtracting 1 nm from the radius of the disc for the diameter of an α-helix (the MSP), and subtracting the area of NTS1 based on a radius of approximately 2 nm, it can be calculated that there are approximately 62 lipid molecules per leaflet (or 70 for empty discs). This is the number of lipid molecules put into the reaction mixture to form nanodiscs for most cases, where a 1:60 MSP:lipid mol ratio was used. This also correlates well with other data indicating a typical lipid number of 62 lipid molecules per leaflet for POPC only discs, where a slightly larger lipid area for POPC was used [15,16]. NTS1 would therefore be surrounded by just over three complete annuli of lipid molecules in the nanodisc. Calculating the number of lipid molecules from the total molecular mass given by the Stoke's radius (200 kDa) would give almost 20 lipid molecules (average MW of 750 Da) more per nanodisc.

3.2. FLAG-NTS1-nanodisc-G protein coupling

G proteins were amine-coupled to the SPR chip or nanodiscs were captured on an L1 chip (Fig. 2A–C). Between 5000 and 13 000 RU were coupled and the surface rigorously washed to minimise baseline drift. Injections of nanodiscs over G protein showed some concentration-dependence in the signal at higher concentrations, which was partially abolished by lowering the top concentration of analyte (Fig. 2A and B). Single cycle kinetics (SCK) programmes were used. Empty nanodiscs were used as a reference in order to match the refractive index of the sample solution, since it contained both protein and lipid. To fit the data, a standard 1:1 Langmuir binding model was used initially, but ultimately, a heterogeneous ligand binding (HLB) model was found to be more appropriate, given the non-specific nature of amine coupling (inbuilt BiaEvaluation software, Biacore). HLB global fits to the single cycle kinetics data produced the kinetic parameters listed in Table 1.

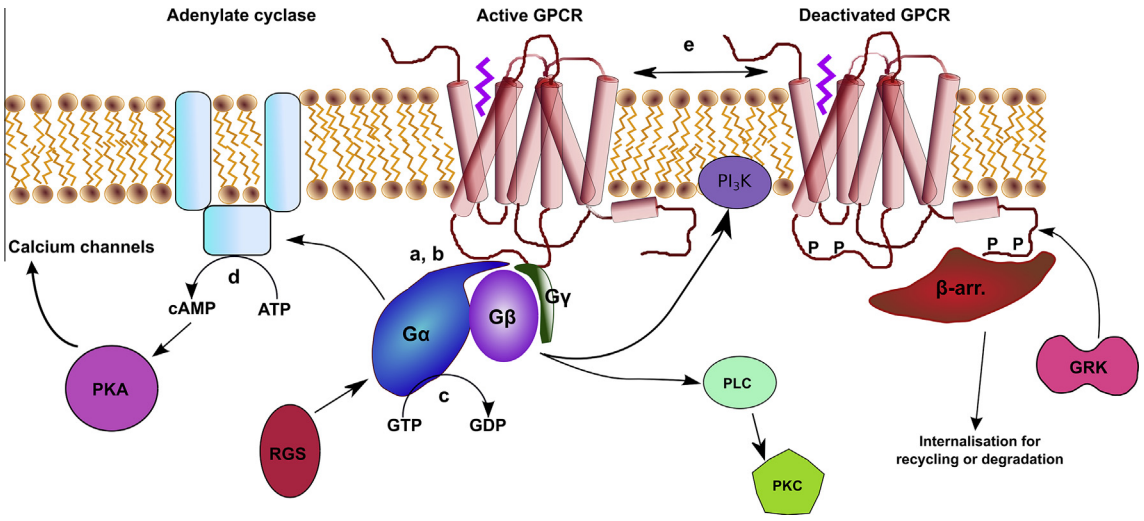

Fig. 3. Kinetics of the GPCR interactome. Some of the initial steps in the GPCR signalling pathway. The GPCR activates a heterotrimeric G protein (a,b) via the GTPase domain of the Gα subunit, which is regulated by regulators of G protein signalling (RGS), causing hydrolysis of GTP to GDP (c). The heterotrimer dissociates into α and βγ subunits. The hydrolysis of ATP to cyclic AMP (cAMP) (d) is catalysed by interactions of Gα with adenylate cyclase, which regulates Ca^{2+} channels via activation of protein kinase A (PKA) by cAMP. The Gβγ subunits activate phosphatidylinositide 3-kinase and phospholipase C (PLC). PLC cleaves phosphatidylinositol 4,5-bisphosphate (PIP_2) into inositol 1,4,5-trisphosphate (IP_3) and diacyl glycerol (DAG) which activate the release of Ca^{2+} from the endoplasmic reticulum and the activation of protein kinase C (PKC). PKA and G protein-coupled receptor kinases (GRKs) phosphorylate the GPCR, leading to coupling of the receptor to arrestin and subsequent down-regulation of the receptor by internalisation for recycling or degradation in lysosomes. (a,b) $G\alpha_{i1}$ and $G\alpha_s$ affinities for NTS1 of 15 ± 6 nM and 31 ± 18 nM (SE), respectively (this study). (c) BODIPY-GTP hydrolysis K_m value was 120 ± 60 nM [55]; GTPγS binding k_{app} = 0.027 min^{-1} [56]. (d) Basal activity ~20–65 pmol cAMP/min/mg [57], k_{obs} of ~$1 \times 10^{-3} - 6 \times 10^{-4}$ s^{-1} [58]. (e) Spontaneous diffusion-interaction on the ms timescale [59], with dissociation rates of 1.3 s^{-1} [60], and a K_D of 2–20 nM [61].

4. Discussion

4.1. GPCR-G protein signalling

For the first time, the direct interactions of a GPCR in nanodiscs with G proteins have been investigated using SPR. The kinetics of this interaction and the affinity of binding are of much interest. These are aspects of G protein coupling, or any downstream events, that have rarely been assayed directly. Typical assays for G protein-GPCR coupling follow the activation of the G protein through radioactive assays using [^{35}S]GTPγS, or by assaying cAMP or Ca^{2+} levels. Knowing the affinity of a G protein for a GPCR, and the differential affinities of the various G proteins for the same GPCR, and then isolating the residues involved in the interaction and potentially studying how different βγ subunits influenced the interaction, would be of immense use for the development of drugs targeting specific signalling pathways or protein-protein interfaces (druggable interfaces). An additional level of complexity that needs to be unravelled would be how different agonists affect the affinities and rates of binding of G proteins to GPCRs, and whether the type of lipid environment of the receptor has any influence on these parameters.

4.2. Novel use of nanodiscs to detect signalling

Reconstituting NTS1 into nanodiscs eliminated bulk signals caused by detergent and/or glycerol, which are required for maintenance of receptor function and stability when extracted from membranes. Drift from the chip was also eliminated, because the receptor itself could be used as the analyte rather than tagged to NT as the ligand. Further advantages of this configuration were that NTS1 was in a bilayer, the nanodiscs could be dialysed and concentrated, and the NTS1-nanodiscs could also be used as the ligand, by capturing them on an L1 chip. Using the empty nanodiscs as the reference "blank" ensured that the closest fitting blank possible was being used to subtract any non-specific binding signal.

4.3. Scope

GPCR structure and function are ideally assayed in a membrane environment [29–31]. However, lipid membranes and membrane-mimetic environments do not readily lend themselves to most biophysical methods. SPR is by now a well-established real-time, label-free means of robustly determining the binding constants and affinities of proteins for antibodies, ligands or other binding partners, and the binding of NTS1 to NT in detergent has already been demonstrated [3,32]. A number of other studies have investigated GPCR-ligand or drug interactions, reconstitution of GPCRs on SPR chips, or GPCR-G protein interactions in detergent [33–41].

Nanodiscs have been used as the analyte in SPR studies previously. Some instances were found [27,42,43], but to date no other SPR study has used nanodiscs to investigate GPCR-G protein coupling. The affinity constants of NTS1 in nanodiscs determined for both $G\alpha_{i1}$ and $G\alpha_s$ were in the low nanomolar range, implying high affinity for the receptor. There was statistically no difference in the affinities, or in the affinity of GTPγS-bound $G\alpha_s$ for the receptor. Reducing heterogeneity in the system may prove this not to be the case, but stable receptor-G protein-GTPγS complexes have been observed [44].

Our experiments were performed in the presence of ligand. However, Alves et al. used plasmon waveguide resonance, a variant of SPR, to study the affinities of various $G\alpha_i$ and $G\alpha_o$ proteins for the δ-opioid receptor in the presence and absence of ligand. The affinities were found to be ligand- and βγ-subunit-dependent [12,45]. Thus, within the setting of the cell there is enormous potential for broad scope of receptor function, depending on multiple parameters. With every additional parameter, sensitivity and subtlety of function grows. GPCRs are able to bind many different ligands and G proteins. If the affinity of each different G protein for the receptor is modulated by the type and presence or absence of ligand, the type and presence or absence of βγ subunit; and the affinity of GTP(γS), which activates the G protein, for the G protein alters according to the above parameters, the scope for function is significant. Add to this the potential for homo- and hetero-dimer-

isation of the receptor and it becomes increasingly clear why GPCRs are responsible for, and capable of controlling, so many of the essential and critical cell functions, and why any defect of function anywhere along the signalling pathway can have such a profound influence on the health of the organism.

The ability to explore, relatively rapidly, the affinities of various G proteins for their cognate receptors is important for many reasons, including testing the effects of mutations to conserved residues within the C-terminal α-helix of the G protein, or within the residues of a GPCR that are expected to bind the G protein, or the effects of different lipid environments on the coupling affinity and rate of binding of a GPCR to G proteins, or the effect of the βγ-subunit on the coupling, is immensely useful for later clinical research for drug-targeting of signalling pathways. These are aspects currently under study.

Mapping the GPCR interactome is going to be challenging due to its inherent complexity [46–48] (Fig. 3), and here we have shown one approach to understanding the biology associated with cellular responses controlled through GPCRs. This importance has not escaped the pharmaceutical industry, as demonstrated through its continuance to focus on GPCRs as drug targets [49–53].

Acknowledgments

Funding for this work was provided by the Wellcome Trust as a studentship for RJA, Corpus Christi College, Oxford, and the Oppenheimer Fund. We would like to acknowledge David Staunton for help with the SPR and Renaud Wagner for the G protein constructs.

Appendix A. Supplementary data

Supplementary data associated with this article can be found, in the online version, at http://dx.doi.org/10.1016/j.febslet.2014.10.043.

References

[1] Downes, G.B. and Gautam, N. (1999) The G protein subunit gene families. Genomics 62, 544–552.
[2] Vincent, J.P., Mazella, J. and Kitabgi, P. (1999) Neurotensin and neurotensin receptors. Trends Pharmacol. Sci. 20, 302–309.
[3] Harding, P.J., Attrill, H., Ross, S., Koeppe, J.R., Kapanidis, A.N. and Watts, A. (2007) Neurotensin receptor type 1: *Escherichia coli* expression, purification, characterization and biophysical study. Biochem. Soc. Trans. 35, 760–763.
[4] Pelaprat, D. (2006) Interactions between neurotensin receptors and G proteins. Peptides 27, 2476–2487.
[5] Dobner, P.R. (2006) Neurotensin and pain modulation. Peptides 27, 2405–2414.
[6] Remaury, A. et al. (2002) Targeted inactivation of the neurotensin type 1 receptor reveals its role in body temperature control and feeding behavior but not in analgesia. Brain Res. 953, 63–72.
[7] Driessen, T.M., Zhao, C., Whittlinger, A., Williams, H. and Gammie, S.C. (2014) Endogenous CNS expression of neurotensin and neurotensin receptors is altered during the postpartum period in outbred mice. PLoS One 9, e83098.
[8] Rasmussen, S.G. et al. (2011) Crystal structure of the beta2 adrenergic receptor-Gs protein complex. Nature 477, 549–555.
[9] White, J.F. et al. (2012) Structure of the agonist-bound neurotensin receptor. Nature 490, 508–513.
[10] Alves, I.D., Cowell, S.M., Salamon, Z., Devanathan, S., Tollin, G. and Hruby, V.J. (2004) Different structural states of the proteolipid membrane are produced by ligand binding to the human delta-opioid receptor as shown by plasmon-waveguide resonance spectroscopy. Mol. Pharmacol. 65, 1248–1257.
[11] Alves, I.D., Park, C.K. and Hruby, V.J. (2005) Plasmon resonance methods in GPCR signaling and other membrane events. Curr. Protein Pept. Sci. 6, 293–312.
[12] Alves, I.D., Salamon, Z., Varga, E., Yamamura, H.I., Tollin, G. and Hruby, V.J. (2003) Direct observation of G-protein binding to the human delta-opioid receptor using plasmon-waveguide resonance spectroscopy. J. Biol. Chem. 278, 48890–48897.
[13] Inagaki, S., Ghirlando, R., White, J.F., Gvozdenovic-Jeremic, J., Northup, J.K. and Grisshammer, R. (2012) Modulation of the interaction between neurotensin receptor NTS1 and Gq protein by lipid. J. Mol. Biol. 417, 95–111.
[14] Grisshammer, R. and Hermans, E. (2001) Functional coupling with Galpha(q) and Galpha(i1) protein subunits promotes high-affinity agonist binding to the neurotensin receptor NTS-1 expressed in *Escherichia coli*. FEBS Lett. 493, 101–105.
[15] Bayburt, T.H., Grinkova, Y.V. and Sligar, S.G. (2002) Self-assembly of discoidal phospholipid bilayer nanoparticles with membrane scaffold proteins. Nano Lett. 2, 853–856.
[16] Denisov, I.G., Grinkova, Y.V., Lazarides, A.A. and Sligar, S.G. (2004) Directed self-assembly of monodisperse phospholipid bilayer nanodiscs with controlled size. J. Am. Chem. Soc. 126, 3477–3487.
[17] White, J.F., Trinh, L.B., Shiloach, J. and Grisshammer, R. (2004) Automated large-scale purification of a G protein-coupled receptor for neurotensin. FEBS Lett. 564, 289–293.
[18] Grisshammer, R., White, J.F., Trinh, L.B. and Shiloach, J. (2005) Large-scale expression and purification of a G-protein-coupled receptor for structure determination – an overview. J. Struct. Funct. Genomics 6, 159–163.
[19] Attrill, H., Harding, P.J., Smith, E., Ross, S. and Watts, A. (2009) Improved yield of a ligand-binding GPCR expressed in *E. coli* for structural studies. Protein Expr. Purif. 64, 32–38.
[20] Harding, P.J., Attrill, H., Boehringer, J., Ross, S., Wadhams, G.H., Smith, E., Armitage, J.P. and Watts, A. (2009) Constitutive dimerization of the G-protein coupled receptor, neurotensin receptor 1, reconstituted into phospholipid bilayers. Biophys. J. 96, 964–973.
[21] Ritchie, T.K., Grinkova, Y.V., Bayburt, T.H., Denisov, I.G., Zolnerciks, J.K., Atkins, W.M. and Sligar, S.G. (2009) Chapter 11 – Reconstitution of membrane proteins in phospholipid bilayer nanodiscs. Methods Enzymol. 464, 211–231.
[22] Greentree, W.K. and Linder, M.E. (2004) Purification of recombinant G protein alpha subunits from *Escherichia coli*. Methods Mol. Biol. 237, 3–20.
[23] Leitz, A.J., Bayburt, T.H., Barnakov, A.N., Springer, B.A. and Sligar, S.G. (2006) Functional reconstitution of Beta2-adrenergic receptors utilizing self-assembling nanodisc technology. Biotechniques 40, 601–602. 604, 606, passim.
[24] Borch, J. and Hamann, T. (2009) The nanodisc: a novel tool for membrane protein studies. Biol. Chem. 390, 805–814.
[25] Bayburt, T.H. and Sligar, S.G. (2010) Membrane protein assembly into nanodiscs. FEBS Lett. 584, 1721–1727.
[26] Banerjee, S., Huber, T. and Sakmar, T.P. (2008) Rapid incorporation of functional rhodopsin into nanoscale apolipoprotein bound bilayer (NABB) particles. J. Mol. Biol. 377, 1067–1081.
[27] Gluck, J.M., Koenig, B.W. and Willbold, D. (2011) Nanodiscs allow the use of integral membrane proteins as analytes in surface plasmon resonance studies. Anal. Biochem. 408, 46–52.
[28] Dickey, A. and Faller, R. (2008) Examining the contributions of lipid shape and headgroup charge on bilayer behavior. Biophys. J. 95, 2636–2646.
[29] Yang, Q., Alemany, R., Casas, J., Kitajka, K., Lanier, S.M. and Escriba, P.V. (2005) Influence of the membrane lipid structure on signal processing via G protein-coupled receptors. Mol. Pharmacol. 68, 210–217.
[30] Soubias, O. and Gawrisch, K. (2012) The role of the lipid matrix for structure and function of the GPCR rhodopsin. Biochim. Biophys. Acta 1818, 234–240.
[31] Oates, J. and Watts, A. (2011) Uncovering the intimate relationship between lipids, cholesterol and GPCR activation. Curr. Opin. Struct. Biol. 21, 802–807.
[32] Harding, P.J., Hadingham, T.C., McDonnell, J.M. and Watts, A. (2006) Direct analysis of a GPCR-agonist interaction by surface plasmon resonance. Eur. Biophys. J. 35, 709–712.
[33] Stenlund, P., Babcock, G.J., Sodroski, J. and Myszka, D.G. (2003) Capture and reconstitution of G protein-coupled receptors on a biosensor surface. Anal. Biochem. 316, 243–250.
[34] Northup, J. (2004) Measuring rhodopsin-G-protein interactions by surface plasmon resonance. Methods Mol. Biol. 261, 93–112.
[35] Minic, J. et al. (2005) Immobilization of native membrane-bound rhodopsin on biosensor surfaces. Biochim. Biophys. Acta 1724, 324–332.
[36] Navratilova, I., Sodroski, J. and Myszka, D.G. (2005) Solubilization, stabilization, and purification of chemokine receptors using biosensor technology. Anal. Biochem. 339, 271–281.
[37] Sen, S., Jaakola, V.P., Pirila, P., Finel, M. and Goldman, A. (2005) Functional studies with membrane-bound and detergent-solubilized alpha2-adrenergic receptors expressed in Sf9 cells. Biochim. Biophys. Acta 1712, 62–70.
[38] Komolov, K.E., Senin, I.I., Philippov, P.P. and Koch, K.W. (2006) Surface plasmon resonance study of g protein/receptor coupling in a lipid bilayer-free system. Anal. Chem. 78, 1228–1234.
[39] Navratilova, I., Dioszegi, M. and Myszka, D.G. (2006) Analyzing ligand and small molecule binding activity of solubilized GPCRs using biosensor technology. Anal. Biochem. 355, 132–139.
[40] Langelaan, D.N., Ngweniform, P. and Rainey, J.K. (2011) Biophysical characterization of G-protein coupled receptor-peptide ligand binding. Biochem. Cell Biol. 89, 98–105.
[41] Navratilova, I., Besnard, J. and Hopkins, A.L. (2011) Screening for GPCR ligands using surface plasmon resonance. ACS Med. Chem. Lett. 2, 549–554.
[42] Borch, J., Torta, F., Sligar, S.G. and Roepstorff, P. (2008) Nanodiscs for immobilization of lipid bilayers and membrane receptors: kinetic analysis of cholera toxin binding to a glycolipid receptor. Anal. Chem. 80, 6245–6252.
[43] Justesen, B.H., Hansen, R.W., Martens, H.J., Theorin, L., Palmgren, M.G., Martinez, K.L., Pomorski, T.G. and Fuglsang, A.T. (2013) Active plasma membrane P-type H+-ATPase reconstituted into nanodiscs is a monomer. J. Biol. Chem. 288, 26419–26429.
[44] Strange, P.G. (2010) Use of the GTPgammaS ([^{35}S]GTPgammaS and Eu-GTPgammaS) binding assay for analysis of ligand potency and efficacy at G protein-coupled receptors. Br. J. Pharmacol. 161, 1238–1249.

[45] Alves, I.D., Ciano, K.A., Boguslavski, V., Varga, E., Salamon, Z., Yamamura, H.I., Hruby, V.J. and Tollin, G. (2004) Selectivity, cooperativity, and reciprocity in the interactions between the delta-opioid receptor, its ligands, and G-proteins. J. Biol. Chem. 279, 44673–44682.
[46] Roux, B.T. and Cottrell, G.S. (2014) G protein-coupled receptors: what a difference a 'partner' makes. Int. J. Mol. Sci. 15, 1112–1142.
[47] Ritter, S.L. and Hall, R.A. (2009) Fine-tuning of GPCR activity by receptor-interacting proteins. Nat. Rev. Mol. Cell Biol. 10, 819–830.
[48] Pétrin, D. and Hébert, T.E. (2012) The functional size of GPCRs - monomers, dimers or tetramers? Subcell. Biochem. 63, 67–81.
[49] Roy, S.J., Glazkova, I., Fréchette, L., Iorio-Morin, C., Binda, C., Pétrin, D., Trieu, P., Robitaille, M., Angers, S., Hébert, T.E. and Parent, J. (2013) Novel, gel-free proteomics approach identifies RNF5 and JAMP as modulators of GPCR stability. Mol. Endocrinol. 27, 1245–1266; Keiser, M.J. et al. (2009) Predicting new molecular targets for known drugs. Nature 462, 175–181.
[50] Smrcka, A.V., Lehmann, D.M. and Dessal, A.L. (2008) G protein betagamma subunits as targets for small molecule therapeutic development. Comb. Chem. High Throughput Screen. 11, 382–395.
[51] Tang, X.L., Wang, Y., Li, D.L., Luo, J. and Liu, M.Y. (2012) Orphan G protein-coupled receptors (GPCRs): biological functions and potential drug targets. Acta Pharmacol. Sin. 33, 363–371.
[52] Ratnala, V.R. and Kobilka, B. (2009) Understanding the ligand-receptor-G protein ternary complex for GPCR drug discovery. Methods Mol. Biol. 552, 67–77.
[53] Scott, C.W. and Peters, M.F. (2010) Label-free whole-cell assays: expanding the scope of GPCR screening. Drug Discov. Today 15, 704–716.
[54] Tang, G., Peng, L., Baldwin, P.R., Mann, D.S., Jiang, W., Rees, I. and Ludtke, S.J. (2007) EMAN2: an extensible image processing suite for electron microscopy. J. Struct. Biol. 157, 38–46.
[55] Jameson, E.E., Roof, R.A., Whorton, M.R., Mosberg, H.I., Sunahara, R.K., Neubig, R.R. and Kennedy, R.T. (2005) Real-time detection of basal and stimulated G protein GTPase activity using fluorescent GTP analogues. J. Biol. Chem. 280, 7712–7719.
[56] Kleuss, C., Raw, A.S., Lee, E., Sprang, S.R. and Gilman, A.G. (1994) Mechanism of GTP hydrolysis by G-protein alpha subunits. Proc. Natl. Acad. Sci. U.S.A. 91, 9828–9831.
[57] Wiegn, P., Dutton, J. and Lurie, K.G. (1993) An enzymatic fluorometric assay for adenylate cyclase activity. Anal. Biochem. 208, 217–222.
[58] Rhee, H.-W., Kim, K.-S., Han, P.-L. and Hong, J.-I. (2010) Label-free fluorescent real-time monitoring of adenylyl cyclase. Bioorg. Med. Chem. Lett. 20, 1145–1147.
[59] Kasai, R.S., Suzuki, K.G.N., Prossnitz, E.R., Koyama-Honda, I., Nakada, C., Fujiwara, T.K. and Kusumi, A. (2011) Full characterization of GPCR monomer–dimer dynamic equilibrium by single molecule imaging. J. Cell Biol. 192, 463–480.
[60] Hern, J.A., Baig, A.H., Mashanov, G.I., Birdsall, B., Corrie, J.E.T., Lazareno, S., Molloy, J.E. and Birdsall, N.J.M. (2010) Formation and dissociation of M1 muscarinic receptor dimers seen by total internal reflection fluorescence imaging of single molecules. Proc. Natl. Acad. Sci. 107, 2693–2698.
[61] White, J.F., Grodnitzky, J., Louis, J.M., Trinh, L.B., Shiloach, J., Gutierrez, J., Northup, J.K. and Grisshammer, R. (2007) Dimerization of the class A G protein-coupled neurotensin receptor NTS1 alters G protein interaction. Proc. Natl. Acad. Sci. U.S.A. 104, 12199–12204.